General Disclaimer

One or more of the Following Statements may affect this Document

- This document has been reproduced from the best copy furnished by the organizational source. It is being released in the interest of making available as much information as possible.

- This document may contain data, which exceeds the sheet parameters. It was furnished in this condition by the organizational source and is the best copy available.

- This document may contain tone-on-tone or color graphs, charts and/or pictures, which have been reproduced in black and white.

- This document is paginated as submitted by the original source.

- Portions of this document are not fully legible due to the historical nature of some of the material. However, it is the best reproduction available from the original submission.

Produced by the NASA Center for Aerospace Information (CASI)

NASA TECHNICAL MEMORANDUM

NASA TM X-73520

NASA TM X-73520

EVALUATION OF FLAT-PLATE COLLECTOR EFFICIENCY UNDER CONTROLLED CONDITIONS IN A SOLAR SIMULATOR

by Susan M. Johnson and Frederick F. Simon
Lewis Research Center
Cleveland, Ohio 44135

NOV 1976
RECEIVED
NASA STI FACILITY
INPUT BRANCH

ABSTRACT

The measured thermal efficiencies of 35 collectors tested with a solar simulator, along with the correlation equations used to generalize the data, are presented in this report. The single correlation used is shown to apply to all the different types of collectors tested, including one with black paint and one cover, one with a selective surface coating and two covers, and an evacuated-tube collector. The test and correlation technique is also modified by using a shield so that collectors larger than the simulator test area can also be tested. This technique was verified experimentally for a shielded collector for which the collector shielded area was 31% of the solar simulator radiation area.

A table lists all the collectors tested, the collector areas, and the experimental constants used to correlate the data for each collector.

EVALUATION OF FLAT-PLATE COLLECTOR EFFICIENCY UNDER

CONTROLLED CONDITIONS IN A SOLAR SIMULATOR

by Susan M. Johnson and Frederick F. Simon

Lewis Research Center

SUMMARY

The measured thermal efficiencies of 35 collectors tested with a solar simulator, along with the correlation method for generalizing these data, are presented in this report. The correlation was found to apply to many different types of collectors, including those with black paint and one cover, those with selective surface coating and two covers, and an evacuated-tube collector, and appears also to apply for "oversized" collectors shielded during test, in which the collector shielded area is no greater than approximately 30% of the solar simulator radiation area.

A table lists all the collectors tested, the collector areas, and the experimental constants used to correlate the data for each collector.

INTRODUCTION

An important aspect of solar heating and cooling research is the determination of the thermal efficiency of flat plate solar collectors of various designs. This report presents a summary of solar-simulator test results for 35 collectors, using correlation methods developed and presented in references 1 and 2. The collector design variables include type of absorber material, absorber coating, type and number of covers, honeycomb material, mirrors, vacuum, and method of tube attachment to the absorber plate.

A majority of the collectors tested were less than or equal to the prescribed length and width of the solar simulator radiation surface, namely 4' × 4'. However, some collectors were larger than the simulator test area.

For such collectors, a reflecting shield was placed over that segment of the collector which extended beyond the solar simulator, thus making the collector "effective" area equal to the simulator radiation area. A test was conducted to verify the correlation equation which was used to generalize data thus obtained (ref. 2).

This report summarizes the experimental results obtained on these 35 collectors tested in the solar simulator.

COLLECTORS TESTED

Presented in Table I is a listing of collectors that were tested in the solar simulator along with some of their characteristics. The collectors are identified by absorber coating material, and the type and number of covers used. Selective surface coatings as listed in this report are a grouping of black nickel, black chrome and copper oxide. Types of absorber plate material along with the method of tube attachment to the absorber plate are also listed. Most of the collectors are of the "conventional" flat plate type, consisting of a cover material, absorber plate, and parallel flow configuration. A few of the collectors presented in this report are a semi-concentrating grooved collectors using a selective and nonselective coating, while still another collector characteristically has a single-tube serpentine flow distribution. There is no particular order in which the collectors are listed. Descriptions of some of the collectors discussed in this report can be found in references 3 to 9.

Table I also lists four different types of collector areas that are used for calculating collector efficiency; they are total area (A_T), the transparent cover area (A_g), the absorber area (A_a) and the effective area (A_e). These values and an explanation of their correlations can be found in reference 2. The effective area of a collector is the area that actually receives the sun's energy. It is equal to the absorber area if there are no obstructions (i.e., strips of metal which cross the width of a collector that supports a cover) to the solar radiation. The constants a_θ, b_θ, and c_θ presented in the table will be discussed later in the results.

EXPERIMENTAL METHOD

Test Facility Description

A drawing of the solar simulator indoor test facility is shown in figure 1 and a detailed description of the facility and its systems are presented in references 1 and 2. This facility is unique in that it enables control of several collector test conditions which would otherwise be uncontrollable if the collector were tested outdoors. These conditions are:

(1) Incident direct radiation-provided by the solar simulator with a controllable flux range of 150 to 350 Btu/hr-ft^2.

(2) Ambient air temperature-held constant by means of a roof exhaust fan.

(3) Wind velocity-attained by a fan which provides a steady-state continuous free convection flow over and around the collector.

(4) Working fluid inlet temperature-controlled by a heat exchanger upstream of the collector to enable attainment of the desired working fluid inlet temperature entering the collector manifold.

(5) Working fluid flow rate-monitored by a turbine flow meter. The collector is mounted on a stand with an adjustable table which enables variations of collector tilt angles and incident angles of radiation.

The flow loop consists of storage and expansion tanks, heater, pump, test collector and piping as shown in figure 2. The storage tank is an 80-gallon residential hot water tank with two electrical immersion heaters. A 50/50 by weight mixture of ethylene-glycol and water is used as the collector working fluid.

Parameters needed to evaluate collector performance are the solar simulator flux, liquid flow rate, ambient temperature, collector fluid inlet and outlet temperatures, and wind velocity. The simulator solar flux level is measured with a water-cooled Gardon type radiometer having a sapphire window, and was calibrated in accordance with the National Bureau of Standards irradiance standard. ISA type E thermocouples are used to measure ambient temperature and collector fluid inlet and outlet temperatures. The thermocouples were calibrated at 32° and 212 $^\circ$ F.

The millivolt-level electrical outputs of the measuring instruments are recorded on magnetic tape by the use of a high-speed data acquisition system. The information from the tape is sent to a digital computer for data reduction and compilation. The computer results are printed out in the test facility within minutes after the data is initially recorded.

Test Procedure

The collector is mounted on the test stand such that the solar simulator radiant flux is normal to the collector. Before the simulator is turned on, the collector is allowed to reach thermal equilibrium at a prescribed flow rate of 10 lbs/hr-ft^2 of absorber area and a prescribed fluid flow inlet temperature. This usually takes about one hour. Once thermal equilibrium is established, the simulator is turned on and set for the appropriate flux level by adjusting the lamp voltage. It will usually take about 15 minutes to obtain a steady-state condition after which data is recorded. The radiant flux is then readjusted to a different value at the same inlet temperature, steady-state conditions obtained, and data again recorded. The inlet temperature of the collector is then set at another value and the process is repeated. Tests are conducted at a flow rate of 10 lb/hr-ft^2, at two different flux levels, and a minimum of three different inlet flow temperatures (between 75° F to 210° F).

COLLECTOR TEST RESULTS

The experimental efficiency of each collector was calculated using the following equation:

$$\eta = GC_p \left(\frac{T_o - T_1}{q_{dr}} \right) \qquad (1)$$

Where G is defined as the flow rate per unit of effective area for solar collection

$$G = \frac{\dot{m}}{A_e} \tag{2}$$

Correlation method. - A detailed discussion of the basis for the following method of correlating collector test data was presented in reference 1. Basically, this method involves the utilization of analytical equations that describe collector efficiency. The equation used for correlating collector efficiency is:

$$\eta = F_R \left\{ \frac{\alpha\tau - \left[\left(\frac{A_a}{A_e} \right) U_L (T_1 - T_a) \right]}{q_{dr}} \right\} \tag{3}$$

Table I indicates that for many collectors the absorber plate is unobstructed, therefore the effective area for solar collection (A_e) is equal to the absorber area $(A_e = A_a)$. For these cases the area ratio shown in equation (3) is unity $(A_a/A_e = 1)$.

From an inspection of equation (3) it can be seen that a correlation of experimental collector performance may be obtained by plotting efficiency versus temperature difference divided by radiant flux (η versus $(T_1 - T_a)/q$).

To account for the effect of temperature on the heat loss coefficient, U_L, equation 3 is expressed as follows to correlate experimental collector performance data:

$$\eta = a_\theta - \left(b_\theta \theta + c_\theta \theta^2 \right) \tag{4}$$

where

$$a_\theta = F_R \alpha_T$$

$$b_\theta + c_\theta \theta = F_R \left(\frac{A_a}{A_e} \right) U_L$$

$$\theta = \frac{T_1 - T_a}{q_{dr}}$$

Constants a_θ, b_θ, and c_θ are presented in Table I and were determined by actual experimental test results.

Shielded collector test. - The use of equation 3 has an advantage in the case where the effective collector area is greater than the area of radiation provided by the solar simulator ($A_e > 16$ ft^2) (see ref. 2). This feature was noted with ten collectors (numbers 14, 17, 19, 23, 29, 30, 31, 32, 33, and 34). With these collectors a reflecting shield was placed over that segment of the collector which extended beyond the solar simulator radiation area, thus, making the effective area equal to the simulator maximum radiation area (16 ft^2).

The effect of the shield is to increase the slope of the correlating equation as indicated by the following equation:

$$\eta' = F_R \left\{ \frac{\alpha_T - \left[\left(\frac{A_a}{A_e'} \right) U_L (T_1 - T_a) \right]}{q_{dr}} \right\} \tag{5}$$

During shielded tests, to enable maintaining a uniform sink temperature for determining collector heat loss and thereby maintaining the same loss coefficient that the collector would have without a reflecting shield, the shield was held at ambient temperature and was positioned 2 inches above the collector. This enables modification of the correlation equation for performance with the shield to obtain the performance equation for the normal case when the collector is unshielded.

Equation 5 indicates that the data on collectors which incorporate a shield can be modified to get the actual slope of the performance curve when the entire collector area is exposed to solar radiation. This modification can be accomplished by multiplying the slopes of the correlating lines by the ratio of the effective collector area with and without the shield (A_e'/A_e). Equation 6 is thus:

$$\eta = F_R \left\{ \frac{\alpha_T - \left[\left(\frac{A_e'}{A_e}\right) U_L (T_1 - T_a) \right]}{q_{dr}} \right\} \tag{6}$$

A test was run on collector 4 to determine the performance both with and without a shield. The fraction of the collector absorber area was shielded for this test was 31%. The performance correlation obtained by use of a shield was modified by employing equation 6, and then comparing the data correlation obtained in that manner with the data correlation of the "no shield" test. Results of these tests (fig. 3) appear to justify, at least for area blockage fractions up to 0.3, the use of a shield and equation 6 for obtaining the performance correlation of a collector that is fully exposed to solar radiation.

Performance curves. - Collector experimental performance curves obtained by use of equation 4 are shown in figures 4 to 10. It can be seen from these figures that no two collectors will perform exactly the same, even though they have generally similar construction.

According to equation 4, the slopes of the curves in figures 4 to 10 represent the heat loss of the collectors. Thus one can compare the heat loss of characteristics the various collectors without actually knowing the specific values of heat loss for each. Collectors 8 and 9 (fig. 4) and collectors 10 and 11 (fig. 5) are identical collectors except for the introduction of a mylar honeycomb between the absorber plate and the transparent cover. This honeycomb material reduces convection and radiation losses, thus reducing the slope of the performance curves.

8

Heat loss can also be reduced by the use of a vacuum. Collector 16 is an evacuated-tubular arrangement, and its low heat loss is clearly shown by the slope of the curve for that collector in figure 6.

The number of covers will also affect the heat loss of a collector. Two covers will decrease the heat loss and cover transmittance to a greater degree than a single cover collector, as shown by collector numbers 32[*] and 35[*] in figure 8.

The intercept on the ordinate of the performance curves is a function of collector plate heat-removal efficiency, F_R, collector surface absorptance, α, and effective transmittance, τ. A comparison of the performance of collectors 7 and 22 in figure 7 indicates that the type of cover plates can make a change in the intercept of a performance curve. Collector 22 was constructed with anti-reflective glass covers which improved the transmittance of solar energy while lower transmittance characteristically of Tedlar decreased the intercept of collector 7. Another example of how transmittance did affect performance of a collector can be shown by comparison of collectors 19, 33, and 34 in figure 6. The three collectors are identical except for the covers. Collector 19 had a high iron oxide content glass (ordinary plate) while the other two collectors, number 33 and 34, had water-white crystal glass which has a lower iron oxide content. A water-white crystal cover has properties of higher transmittance and lower absorptance losses than the ordinary plate glass. Thus, it contributed favorably to an improved intercept value and efficiency curve.

Figure 8 presents the performance of collectors 25 to 28, 32 and 35. Mirrors were installed on the black paint absorber surface of collector 26 and on the black nickel absorber surface of collector 28 to determine the effect upon performance. Figure 8 indicates that the performance collectors 26 and 28 with mirrors falls below that of collectors 25 and 27 without mirrors. This occurred because the mirrors absorbed thermal energy from the absorber plate, then radiating the energy to the surrounding space (see ref. 2).

Both collectors 32 and 35 had proprietary coatings and therefore were not

---

[*]Note: These two collectors are listed as having proprietary coatings; visual inspection seems to indicate they are probably of a selective coating category.

catagorized with the known coatings. Collector 32 had two glass covers while collector 35 had one cover. Collector 35 had a single-tube serpentine flow distribution instead of the usual parallel flow configuration.

Figures 9 and 10 presents a summary of the performance characteristics of collectors tested to date, along with a notation of the source (manufacturer and/or distributor). Figures 9 and 10 present the selective surface and nonselective collectors, respectively. Since a collector may have one or more functions to perform when it is installed in a home or building, it is important to evaluate collector efficiency in light of the specific purpose or function for which it is intended. Abscissa values near the ordinate (again in figs. 9 and 10) are usually representative of pool heating and these collector efficiencies are seen to be in the range of 45 to 85%. Solar air conditioning corresponds to about 0.6 on the abscissa, with available collector efficiencies shown to be in the range of 0 to 50%. This illustrates that the same collector that is good for pool heating will not necessarily perform well for an air conditioning function. Conversely, the expensive construction required to obtain good, high temperature performance required for solar air conditioning is not needed for pool heating. Thus, efficiency alone is not a figure of merit; cost and application must also be considered.

As a final note, figures 4 to 10 show that no two collectors have the same performance curves, even for cases where the same types of coatings, absorber panel material, and number and types of cover plates are used.

SUMMARY OF RESULTS

The performance curves of 35 collectors tested in a solar simulator are presented in this report along with thermal efficiency correlations derived and used to obtain these curves. This data correlation can be used for collectors with (1) black paint and one cover, (2) black paint and two covers, (3) selective surface coating and one cover, and (4) selective surface coating and two covers. The correlation appears to hold for collector designs of considerable variation, including those such as a vacuum, honey-

combs, anti-reflective glass, various tube bonding methods, side mirrors, and various types of cover plate materials such as glass, Tedlar, and Lexan.

The efficiency of each collector could be represented by a single line. The majority of these lines fell within a given bandwidth (of 65 to 75%) at the ordinate intercept. It was also noticeable in the figures that no two collectors had the same performance curves, even though the same types of coatings and cover plates were used.

With collectors which have effective areas greater than the area of radiation of the solar simulator, a reflecting shield must be placed over that segment of the collector which extends beyond the solar simulator radiation area. With the shielded collectors, correlations equations 3 and 6 appear to apply if the shielded area is no greater than 30% of the solar simulator radiation area.

SYMBOLS

A_a absorber area, ft^2

A_e' effective collector area with shield, ft^2

A_e effective collector area, ft^2

A_g transparent cover area, ft^2

A_T total collector area, ft^2

C_p fluid heat capacity, Btu/lb, ^oF

F_R collector plate heat-removal efficiency, dimensionless

G flow rate of collector fluid, lb/hr-sq ft of absorber surface

$\dot{m}$ flow rate, lb/hr

q_{dr} incident direct solar radiation, Btu/hr-ft^2 (in collector plane)

T_a ambient temperature, ^oF

T_o fluid outlet temperature, ^oF

T_1 fluid inlet temperature, ^oF

U_L overall collector heat loss coefficient, Btu/hr-ft^2, ^oF

α collector surface absorptance, dimensionless

η collector efficiency, dimensionless

τ effective transmittance, dimensionless

REFERENCES

1. F. F. Simon, and P. Harlamert, Flat-Plate Collector Performance Evaluation, The Case for a Solar Simulation Approach. NASA TM X-71247 (1973).

2. F. F. Simon, Flat-Plate Solar-Collector Performance Evaluation with a Solar Simulator as a Basis for Collector Selection and Performance Prediction. NASA TM X-71793 (1975).

3. Power Systems Division, Standardized Performance Tests of Collectors of Solar Thermal Energy - Prototype Moderately Concentrating Grooved Collectors. NASA TM X-71863 (1976).

4. Power Systems Division, Standardized Performance Tests of Collectors of Solar Thermal Energy - Revere Flat-Plate Collector with Two Transparent Covers. NASA TM X-71854 (1975).

5. Power Systems Divisions, Standardized Performance Tests of Collectors of Solar Thermal Energy - A Selectively Coated, Flat-Plate Copper Collector with One Transparent Cover and a Tube-to-Tube Spacing of 3-7/8 Inches. NASA TM X-71868 (1976).

6. Power Systems Divisions, Standardized Performance Tests of Collectors of Solar Thermal Energy - A Steel Flat-Plate Collector with Two Transparent Covers and a Proprietary Coating. NASA TM X-71869 (1976).

7. Power Systems Division, Standardized Performance Tests of Collectors of Solar Thermal Energy - A Selectively Coated, Steel Collector with One Transparent Cover. NASA TM X-71870 (1976).

8. Power Systems Division, Standardized Performance Tests of Collectors of Solar Thermal Energy - A Selectively Coated, Flat-Plate Copper Collector with One Transparent Cover and a Tube-to-Tube Spacing of $5\frac{5}{8}$ Inches. NASA TM X-71871 (1976).

9. S. Johnson, Standardized Performance Tests of Collectors of Solar Thermal Energy - A Flat-Plate Collector with a Single-Tube Serpentine Flow Distribution. NASA TM X-73417 (1976).

TABLE I. - COLLECTORS TESTED

Number	Collector	Absorber material	Collector area, A_T, sq ft	Cover area, A_g, sq ft	Absorber area, A_a, sq ft	Effective area, A_e, sq ft	a_θ	b_θ	c_θ	
1	Black paint-2 glass	Cu (1)	16.3	15	13.8	13.8	0.75	0.833	0	1
2	CuO-1 glass	Cu (2)	8.6	6.9	6.9	6.9	.795	1.17	0	2
3	CuO-1 glass, Al. honeycomb	Cu (2)	8.6	6.9	6.9	6.9	.795	1.17	0	3
4	CuO-2 glass	Cu (2)	8.9	8	7.9	7.9	.59	.76	0	4
5	Black nickel-2 glass	Al (1)	16	15	13.5	13.5	.713	.504	0.14	5
6	Black nickel-1 tedlar		7.9	7.4	6.1	5.7	.567	.755	.141	6
7	Black nickel-2 tedlar		7.9	7.4	6.1	5.7	.533	.642	.0729	7
8	Black paint-1 glass		16	15	13.5	13.5	.850	1.139	.161	8
9	Black paint-mylar honeycomb-1 glass						.817	.806	.119	9
10	Black paint-mylar honeycomb-2 glass						.735	.497	.284	10
11	Black paint-2 glass						.728	.705	.251	11
12	Black paint-2 glass					11.80	.748	.719	.197	12
13	Black paint-2 glass	Steel (4)	----	----	14.9	14.9	.701	.548	.601	13
14	Black paint-2 glass	Al (1)	18.1	17.9	17.9	17.9	.615	.954	.013	14
15	CuO-1 glass-1 Lexan	Cu (2)	12	10.8	10	10	.574	.837	.141	15
16	Selective surface-glass-evacuated-tube	Glass	14.4	21.6	17.4	17.4	.45	.24	0	16
17	Selective surface-2 glass	Al (1)	27.9	24.8	23	22	.665	.648	.0007	17
18	Black paint-1 glass	Cu (3)	12	9.6	10.5	9.3	.593	1.153	.0861	18
19	Black nickel-1 glass	Steel (2)	19.1	15.6	15.7	15.3	.689	.976	.125	19
20	Selective surface-2 glass	Steel (4)	6.3	5.5	5.3	5.3	.433	.718	.175	20
21	Black chrome-2 glass	Steel (4)	16	15	13.3	13.3	.725	.687	.050	21
22	Black nickel-2 AR glass	Al (1)	16	15	13.5	13.5	.85	.626	0	22
23	Selective surface-2 lexan		25.3	23.2	22.9	22.9	.673	.695	0	23
24	Black paint-2 glass		18.52	17.95	17.56	17.56	.638	.832	0	24
25	Black paint-2 glass		9.0	8.3	5.9	5.4	.53	.64	0	25
26	Black paint-2 glass with mirrors				3.24	2.97	.54	1.00	0	26
27	Black nickel-2 glass				5.9	5.4	.52	.575	0	27
28	Black nickel-2 glass with mirrors				3.24	2.97	.43	.533	0	28
29	Selective surface-1 glass	Cu (2)	25.68	22.55	22	22	.684	.835	0	29
30	Selective surface-1 glass	Cu (2)	16.0	14.32	13.8	10.89	.658	.82	0	30
31	Black paint-2 glass	Cu (5)	19.6	17.2	16.3	16.3	.720	.956	0	31
32	Proprietary-2 glass	Steel (3)	20.40	17.32	17.06	16.94	.674	.76	0	32
33	Black nickel-1 glass	Steel (2)	19.01	16.23	15.4	14.95	.744	.95	0	33
34	Black nickel-1 glass	Steel (2)	18.60	15.59	15.96	15.50	.731	.9125	0	34
35	Proprietary-1 glass	--------	16.0	14.45	13.75	13.37	.848	1.075	0	35

[1] Tube sheet.
[2] Tubes bonded to absorber plate.
[3] Tubes clamped to absorber plate.
[4] Tubes spot welded absorber plate.
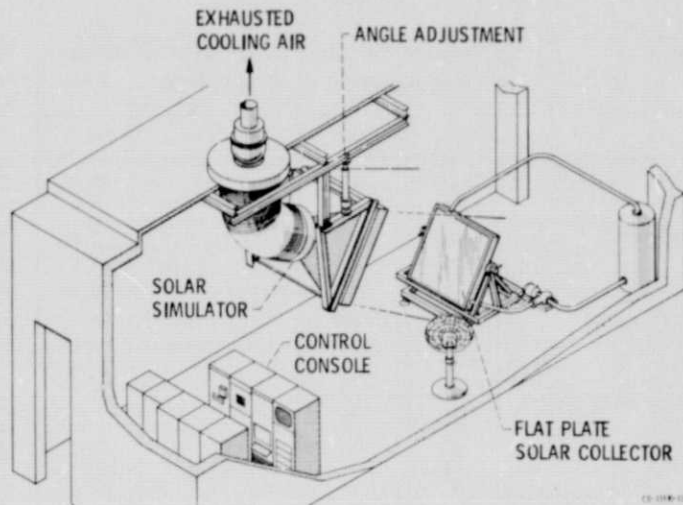[5] Tubes bonded and clamped to absorber plate.
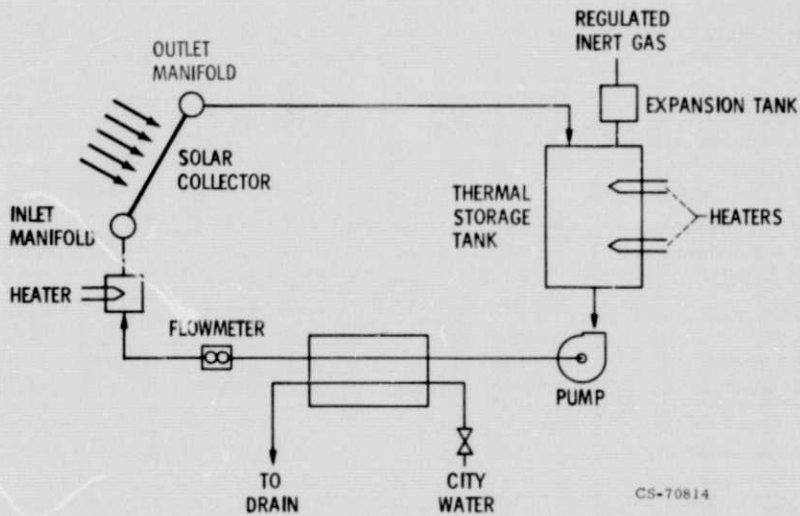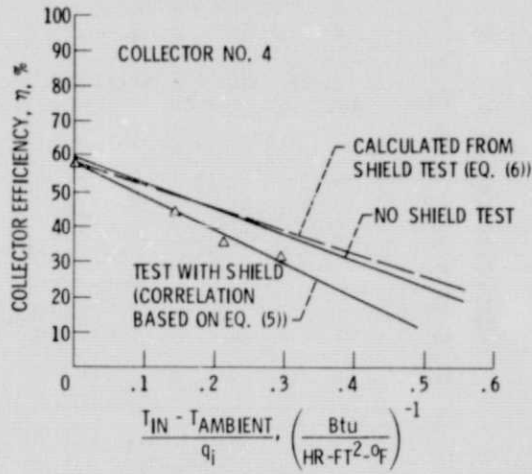
Figure 1. - Solar simulator indoor test facility.

Figure 2. - Schematic of liquid flow loop.

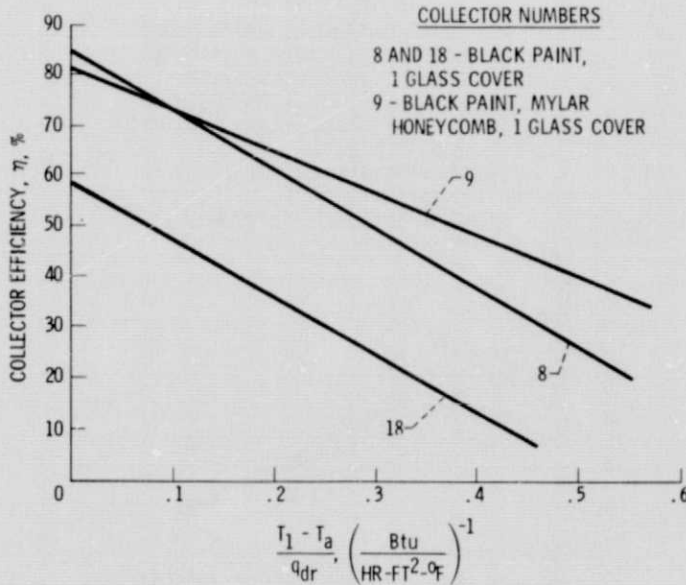Figure 3. - Effect of collector shading on performance correlation.

Figure 4. - Zero incidence performance curves for black paint - one cover collector.

1, 11-14, 24, 25 AND 31 - BLACK PAINT,
WITH 2 GLASS COVERS

10 - BLACK PAINT MYLAR HONEYCOMB
WITH 2 GLASS COVERS

CS-77494
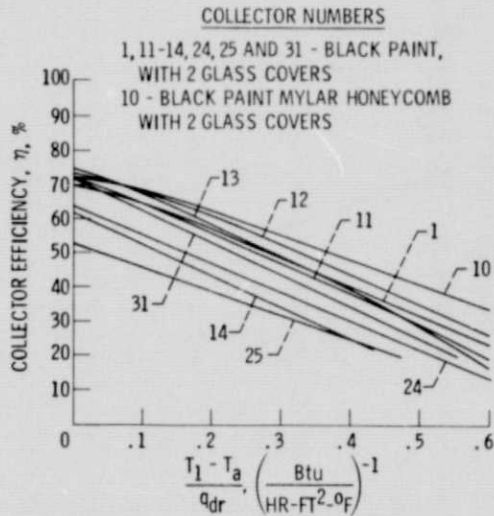
Figure 5. - Zero incidence performance curves for
black paint - two cover collector

COLLECTOR NUMBERS

2 - COPPER OXIDE WITH 1 GLASS COVER
3 - COPPER OXIDE, HAVING AN ALUMINUM
HONEYCOMB WITH 1 GLASS COVER
6 - BLACK NICKEL WITH 1 TEDLAR COVER
16 - SELECTIVE SURFACE-GLASS-EVACUATED
TUBULAR COLLECTOR
19, 33, AND 34 - BLACK NICKEL WITH
1 GLASS COVER
29 AND 30 - SELECTIVE SURFACE WITH
1 GLASS COVER

CS-77496
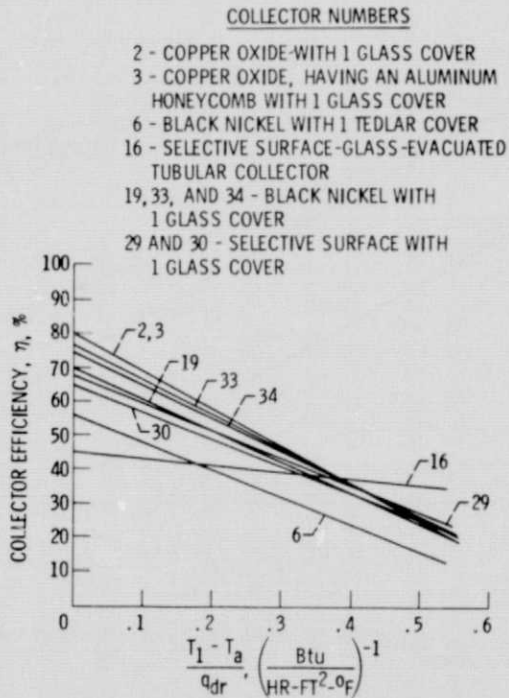
Figure 6. - Zero incidence performance curves for
selective surface - one cover collectors.

COLLECTOR NUMBERS

4 - COPPER OXIDE WITH 2 GLASS COVERS
5 AND 27 - BLACK NICKEL WITH 2 GLASS COVERS
7 - BLACK NICKEL WITH 2 TEDLAR COVERS
15 - COPPER OXIDE WITH 1 GLASS COVER AND
1 LEXAN COVER
17 AND 20 - SELECTIVE SURFACE WITH
2 GLASS COVERS
21 - BLACK CHROME WITH 2 GLASS COVERS
22 - BLACK CHROME WITH 2 ANTIREFLECTIVE
GLASS COVERS
23 - SELECTIVE SURFACE WITH 2 LEXAN COVERS
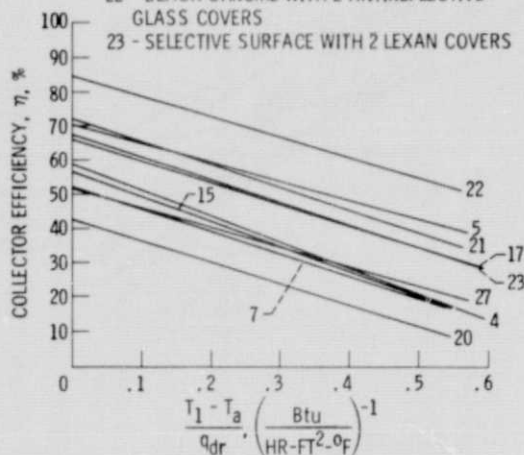
CS-77495

Figure 7. - Zero incidence performance curves for
selective surface - two cover collectors.

COLLECTOR NUMBERS

25 - BLACK PAINT WITH 2 GLASS COVERS
26 - BLACK PAINT WITH 2 GLASS COVERS
AND MIRRORS
27 - BLACK NICKEL WITH 2 GLASS COVERS
28 - BLACK NICKEL WITH 2 GLASS COVERS
AND MIRRORS
32 - PROPRIETARY COATING WITH 2 GLASS COVERS
35 - PROPRIETARY COATING WITH 1 GLASS COVER
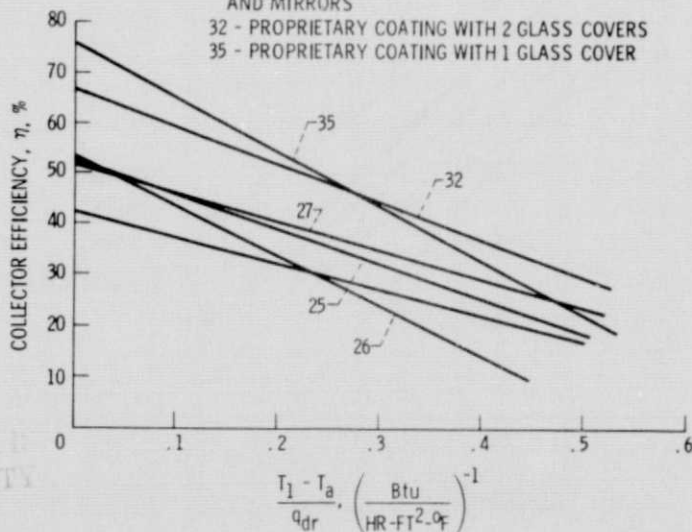
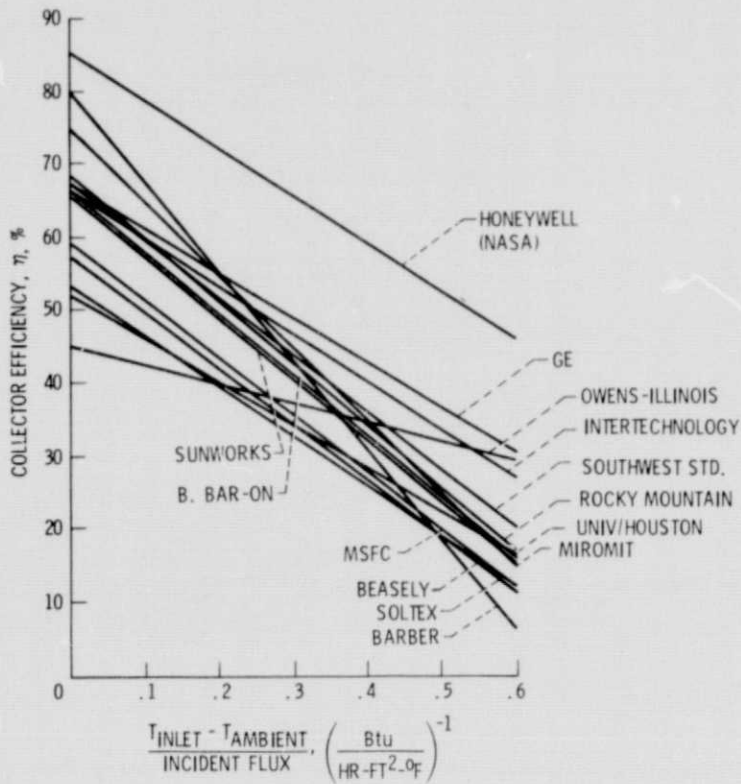Figure 8. - Comparison of some different types of collectors tested.

Figure 9. - Performance characteristics of a group of selective surface collectors.
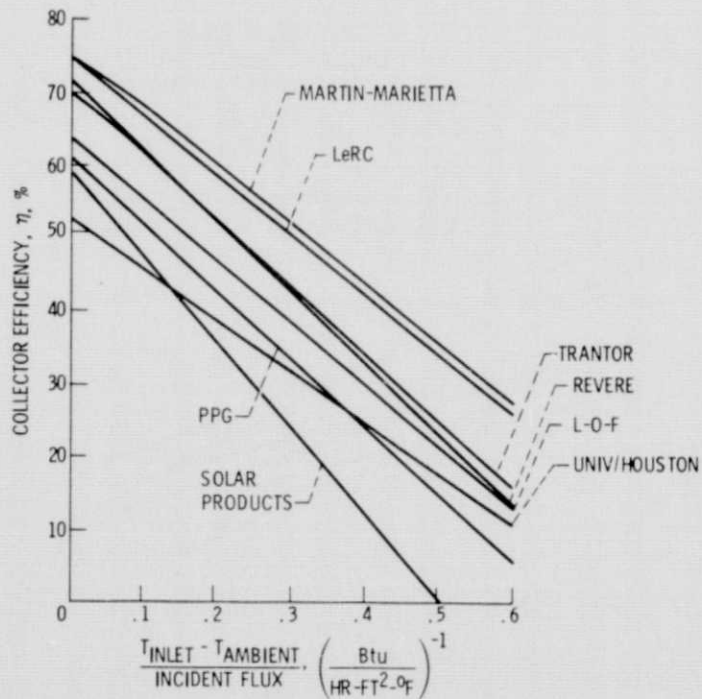

Figure 10. - Performance characteristics of a group of nonselective surface collectors.